Two-Dimensional Solid State NMR and Separation of ^{7}Li Quadrupolar Interactions in Paramagnetic Compounds

S. Ganapathy, P. R. Rajamohanan, and P. Ganguly*

Physical Chemistry Division, National Chemical Laboratory, Pune 411 008, India

T. N. Venkatraman and Anil Kumar

Sophisticated Instruments Facility, Indian Institute of Science, Bangalore 560 012, India

Received: May 15, 1998; In Final Form: October 14, 1998

In layered paramagnetic compounds, such as $La_2Li_{0.5}Ni_{0.5}O_4$ with a perovskite structure, the ^{7}Li NMR spectrum is broadened by anisotropic quadrupolar as well as paramagnetic dipolar interactions. We have used a two-dimensional spin echo (SE) experiment to separate the quadrupolar interaction and obtain a clean quadrupolar spectrum along the ω_1 dimension. This is demonstrated in $La_2Li_{0.5}B_{0.5}O_4$ (B = Cu, Ni), through 2D SE experiments conducted in static samples as well as those in spinning at the magic angle. A quadrupole coupling constant of 92 kHz is estimated from the ω_1 spectrum for paramagnetic $La_2Li_{0.5}Ni_{0.5}O_4$.

1. Introduction

The quadrupolar broadened one-dimensional solid-state NMR spectra carry rich information about the nature of anisotropic interactions present in the system[1]. The determination of correct interaction parameters, such as quadrupole coupling constant and the asymmetry parameter, is often carried out by line shape simulations and comparison of the simulations with the experimental spectra. In the presence of additional line broadening interactions, such as chemical shielding, dipolar interactions, paramagnetic interactions, etc., the line shape simulations involve consideration of a dual axes system in which the interaction tensors can be coincident or noncoincident, the latter one being more general in nature.[2] Systems experiencing quadrupolar and anisotropic magnetic interactions were studied by Siminovitch et al.[3] and France,[4] for integer ($I = 1$) and half-integer spin ($I = {}^7/_2$) cases, respectively. France[4] has presented a recipe to extract the quadrupole and magnetic shielding by noting the powder singularity features, such as steps and shoulders, when they are observed in the experimental spectra.

There are two primary reasons for carrying out these studies. The first concerns the qualitative features of the NMR spectra when the principal axes of the interaction tensors are not coincident. The spectral features may resemble second order quadrupole effects associated with the $I = {}^3/_2$ nucleus and affect the quantitative interpretation of the spectra. Second, when the powder pattern lacks characteristic features such as steps and shoulders, the iterative computer simulation procedure becomes tedious. Further, they are unlikely to lead to the extraction of a unique set of the correct interaction parameter.

The two-dimensional separation techniques have been employed in solid-state NMR spectroscopy to separate dual interactions, such as, chemical shift anisotropy and heteronuclear proton dipolar interaction.[5] These techniques are useful since they achieve a clean separation of the desired interaction from complex NMR spectra by resolving the spectral information along two orthogonal dimensions and effective in determining their mutual orientations.[6] The 2D separation experiments have been reported for both spin $^1/_2$ and quadrupolar [$I = 1$, $((2n + 3)/2)$] nuclei.[6−8] Einnorson et al.[8] have used two-dimensional quadrupolar and spin echo techniques to determine the homogeneous line width, free from broadening due to the magnetic field inhomogenity and orientation distribution of helical axes in macroscopically oriented DNA fibers. They studied the NMR of metal counterions (^{7}Li, ^{133}Cs) in hydrated oriented B-DNA fibers and gathered information about the molecular dynamics of these ions. Furo et al.[9] applied the two-dimensional quadrupole echo method for ^{23}Na nuclei in anisotropic liquids exhibiting small quadrupole splittings. Dolenisek[10] employed the 2D technique in $Rb_{1-x}(NO_4)_xD_2PO_4$ ($x = 0.44$), using the ($-{}^1/_2 \leftrightarrow {}^1/_2$) central transition of ^{87}Rb.

Recently, Terao and co-workers[11] have carried out deuterium 2D MASS NMR of paramagnetic compounds with selectively deuterated acetate groups. In such cases, it is advantageous to separate out the contribution from quadrupolar and paramagnetic interactions by using two-dimensional representation of the spin echo experiment or a three-pulse sequence. The principal values of the interaction tensors were calculated from the projections of the two-dimensional spectrum onto the corresponding diagonals and their mutual orientations from the simulations of the 2D spinning sideband patterns. Pines and co-workers[12] have recently determined the quadrupolar and chemical shift tensors, as well as their relative orientation, using switched-angle spinning (SAS) 2D NMR.

In paramagnetic systems of $((2n + 3)/2)$ quadrupolar nuclei, such as ^{7}Li, the magnitude of the electron−nuclear dipolar interaction is sufficiently large that the observed NMR spectrum exhibits a complex powder line shape. In the layered oxides of the type $La_2Li_{0.5}B_{0.5}O_4$, where B is a paramagnetic ion such as low-spin Ni^{3+}, the anisotropic distribution of the paramagnetic ion in the *ab* plane gives rise to additional anisotropic paramagnetic interaction. The principal axis of the anisotropic paramagnetic dipolar interaction tensor is expected to be

* Author to whom correspondence should be addressed. Present Address: Materials and Structures Laboratory, Tokyo Institute of Technology, 4259 Nagatsuta, Midori, Yokohama 226 8503, Japan.

10.1021/jp9822384 CCC: $19.00
Published on Web 02/19/2000

noncoincident with the unique axis of the electric field gradient for the case B = Ni^{3+}. This introduces an orientation-dependent broadening, governed by these interactions, resulting in an asymmetric ^7Li line shape.[13]

In this paper, we have extended the classical CPMG spin echo sequence to achieve a two-dimensional separation of the quadrupolar interaction from the combined effects of quadrupolar and paramagnetic dipolar interactions in the layered compound $La_2Li_{0.5}Ni_{0.5}O_4$. The separation has been achieved both in a static sample as well as in a sample spinning at the magic angle.

2. Experimental Section

To separate the quadrupolar interaction, we have used the spin echo $\pi/2-t_1/2-\pi-t_1/2-AQ(t_2)$ sequence,[14,15] in which the incremental (t_1) period constitutes the evolution period for ^7Li magnetization. A spin echo is formed due to the refocusing of the anisotropic and inhomogeneous paramagnetic dipolar interactions by the π pulse, as explained below. Since first-order quadrupolar interaction is not affected by the π pulse, the spin echo is modulated by the spin evolution under a quadrupolar Hamiltonian. A sequential incrementation of t_1 from experiment to experiment and accumulation of the FID signal at each t_1 generates the 2D data matrix $S(t_1,t_2)$, which upon double Fourier transformation leads to a two-dimensional frequency domain spectrum $S(\nu_1,\nu_2)$. We have incorporated both F_1 quadrature detection, axial peak suppression, and CYCLOPS[16] into the basic 2D SE sequence. For experiments performed under MAS, the t_1 dwell time was not rotor synchronized so that the F_1 spectral width is not limited by the spinning speed. As a result, a sideband pattern appears along the F_1 dimension also. The 2D data were processed by using a magnitude mode calculation in both the dimensions.

The 2D experiments were performed at the ^7Li Larmor frequency of 116.64 MHz on a Bruker MSL-300 FT-NMR spectrometer. Static experiments were carried out using a wide-line probe housing a small diameter (6 mm) rf coil made from flattened copper wire. This arrangement gave a $\pi/2$ pulse of 3.1 μs using the low power mode of operation on the spectrometer. The MAS spectra were recorded using broad-band CP-MAS probe, the tuning range of which was extended to 116.64 MHz by adding a series capacitor to the X-channel tuning capacitor. A $\pi/2$ pulse of 3.3 μs was achieved for the MAS experiments.

Relevant 2D acquisition and processing parameters are included in figure captions. The layered oxide compounds were prepared by the usual ceramic method as published earlier.[13]

3. Results and Discussion

3.1. Theoretical Basis for 2-D Separation from SE Experiment. In what follows, a simple theoretical basis for the 2D separation of the quadrupolar interaction of ^7Li from combined effects of quadrupolar and paramagnetic dipolar interactions is presented.

The ^7Li NMR spectra of $La_2Li_{0.5}Ni_{0.5}O_4$ are broadened by quadrupolar interactions experienced by the ^7Li nucleus and the paramagnetic dipolar interactions between the ^7Li and Ni^{3+}($S = {}^1/_2$). The quadrupolar interaction arises due to nonvanishing electric field gradients, and this gives rise to the second-order broadening of the central ($-{}^1/_2 \leftrightarrow {}^1/_2$) transition as well as the first-order broadening of the satellite ($+{}^3/_2 \leftrightarrow +{}^1/_2$) transitions. Therefore, we can write for the total Hamiltonian,

$$\mathbf{H} = \mathbf{H}_Z + \mathbf{H}_Q + \mathbf{H}_P \tag{1}$$

where $\mathbf{H}_Z$ is the Zeeman Hamiltonian, $\mathbf{H}_Q$ is the quadrupolar Hamiltonian, and $\mathbf{H}_P$ is the paramagnetic dipolar Hamilonian. The Zeeman interaction has the usual form

$$\mathbf{H}_Z = -\gamma(h/2\pi)H_oI_Z \tag{2}$$

and the quadrupole interaction, written in the principal axis system of the quadrupole tensor,[17] is

$$\mathbf{H}_Q = [e^2qQ/h4I(2I-1)][3I_Z{}^2 - I(I+1)] \tag{3}$$

In eq 3, the various symbols have their usual meaning.

In $La_2Li_{0.5}Ni_{0.5}O_4$, the paramagnetic dipolar interactions arise from the dipole−dipole interactions between the observed ^7Li nucleus and the net paramagnetic moment associated with the Ni^{3+} ($S = {}^1/_2$). The spin states $|\alpha\rangle$ and $|\beta\rangle$ of the electron spin are not long-lived since the electronic relaxation is very rapid on the NMR time scale. Therefore, it is necessary to consider a thermally averaged classical electron magnetic moment $\langle\mu\rangle$, resulting from the fast relaxing electron spins. The induced paramagnetic shift on the observed ^7Li NMR spectrum then can be written as[18,19]

$$H_P = \sum_K \langle\boldsymbol{\mu}\rangle^+ \mathbf{D}_K \boldsymbol{I} \tag{4}$$

where the $\sum_K$ represents contributions due to identical electron moments at various locations around the observed ^7Li nucleus. Here, **D** is the dipolar coupling tensor, and is traceless if electron **g** tensor is taken to be isotropic. The angular dependence for the paramagnetic coupling is embedded through the different crystallite orientations in a powder sample. The central line is shifted by an amount ν_P, which is given by[19]

$$\nu_P = [(\nu_o\beta^2\mu^2)/3K_BT] \sum_k (1 - 3\cos^2\theta_k) r_k{}^{-3} \tag{5}$$

The observed powder pattern is accounted for by eq 5 through θ, which specifies the orientation of the dipolar vector with respect to the magnetic field. When quadrupolar interactions and paramagnetic dipolar interactions are present, as in $La_2Li_{0.5}Ni_{0.5}O_4$, the ^7Li NMR spectral frequencies and intensities are determined by the quadrupolar and paramagnetic dipolar interaction parameters and the mutual orientation of the two tensors. Since the interaction (eq 4) is linear in the spin variable I_Z and behaves inhomogeneously, in a manner similar to chemical shielding.

In the 2D SE sequence $\pi/2-t_1/2-\pi-t_1/2-AQ(t_2)$, the effect of the refocusing π pulse is to eliminate the action of all parts of the total Hamiltonian which are linear in I_Z spin variable. The chemical shift, implicitly included in eq 2, is refocused by the π pulse. As mentioned above, the form of paramagnetic dipolar interaction is analogous to a chemical shielding interaction where the paramagnetic coupling tensor takes the place of the usual diamagnetic shielding tensor. Therefore, these interactions also lead to an inhomogeneous broadening and the π pulse is known to refocus such an inhomogeneous broadening. The quadrupolar interaction is unaffected in the evolution period t_1, while the spin system is subjected to the full Hamiltonian (eq 1) during the detection period t_2. Thus, it can be seen that the quadrupolar part of the interaction, not refocused by the π pulse, can be separated along the ω_1 dimension by using the 2D SE sequence.

3.2. 1D NMR of $La_2Li_{0.5}B_{0.5}O_4$ Systems (B=Cu, Ni). The 1D ^7Li NMR spectrum of the diamagnetic compound $La_2Li_{0.5}Cu_{0.5}O_4$ is shown in Figure 1a. We have used a quad-echo

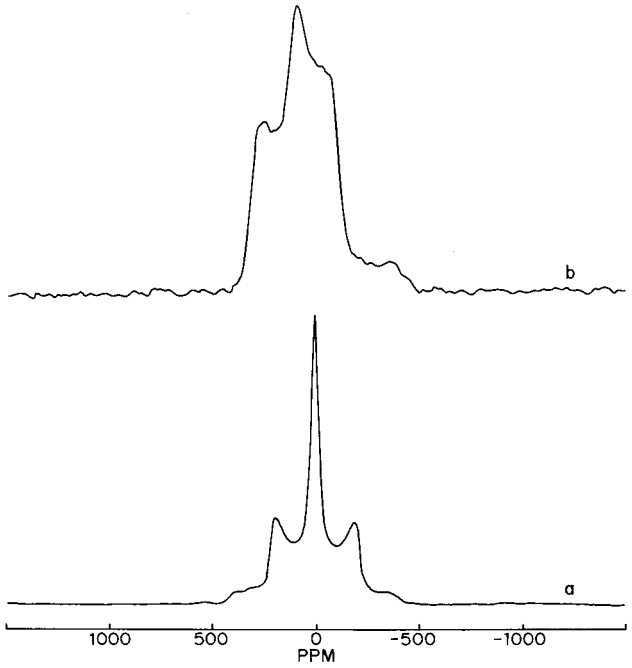

Figure 1. 116.64 MHz static ^{7}Li NMR spectra of $La_2Li_{0.5}B_{0.5}O_4$ system: (a) $La_2Li_{0.5}Cu_{0.5}O_4$ (B = Cu); (b) $La_2Li_{0.5}Ni_{0.5}O_4$ (B = Ni). These spectra were obtained using a quad-echo (QE) sequence using 40 μs τ delay, 2 s relaxation delay, and 500 kHz spectral width. An exponential line broadening of 500 Hz was used prior to Fourier transformation.

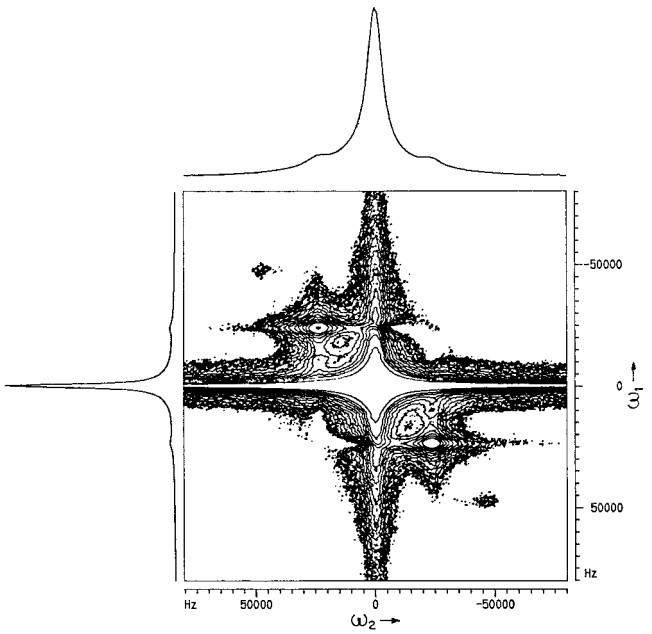

Figure 2. ^{7}Li 2D spin echo (SE) contour plot of $La_2Li_{0.5}Cu_{0.5}O_4$, obtained with a static sample. A 512 (t_1) $\times$1024 (t_2) 2D data matrix was aquried using 250 kHz spectral width, 2 μs t_1 increment, 0.1 s relaxation delay, and 200 scans. The 2D data set was apotized with an exponential line broadening, in the t_1 and t_2 dimensions prior to Fourier transformation. The ω_2 and ω_1 projections are also shown.

sequence $[(\pi/2)_x-\tau-(\pi/2)_y-\tau-\text{echo}]$[20] which removes dead time problems and allows observation of undistorted quadrupolar line shapes.[21] The observed powder pattern is characteristic of a spin $^3/_2$ nucleus experiencing a quadrupolar interaction in an axially symmetric field gradient. From the discontinuities observed for the $\theta = 90°$ at $\pm$22.2 kHz and $\theta = 0°$ at $\pm$ 44.5 kHz, we readily estimate the quadrupole coupling constant to be 88.9 kHz.

The influence of paramagnetic dipolar interaction on the quadrupolar broadened spectrum is seen in the case of ^{7}Li NMR spectrum of $La_2Li_{0.5}Ni_{0.5}O_4$ (Figure 1b). The symmetrical quadrupolar features are no longer seen for this compound. This arises due to the presence of an additional paramagnetic dipolar interaction of comparable magnitude. The spectral frequencies are determined not only by the strength of the quadrupole and dipolar interaction tensors but also by their mutual orientation in a molecule fixed axis system.[2] The determination of quadrupole interaction parameters (e^2Qq/h, η) requires a line shape simulation that takes into account the dual axes system description and a knowledge of the dipolar tensor. In the case of $La_2Li_{0.5}Ni_{0.5}O_4$, the field gradient is due to the elongation of LiO_6 octahedra along the *c* axis, and the Li$-$Ni dipolar interaction vector, due to the presence of Ni $^{3+}$ in the basal plane,[13] is oriented with respect to the efg frame. This results in an asymmetric displacement of the ($\pm$3/2 $\leftrightarrow$ $\pm$1/2) satellite transitions with respect to the central transition, giving rise to the observed ^{7}Li line shape in Figure 1b.

3.3. 2D-NMR of $La_2Li_{0.5}Cu_{0.5}O_4$. The 2D separation experiment using SE sequence was first performed $La_2Li_{0.5}Cu_{0.5}O_4$. The 2D contour plot, together with the ω_1 and ω_2 projections, is shown in Figure 2. Since quadrupolar interactions alone are present for this diamagnetic compound, they are unaffected by the π pulse. Thus, only the quadrupolar Hamiltonian is operative both during the evolution (t_1) and detection (t_2) periods. A 2D Fourier transformation and projection therefore gives rise to the same quadrupolar pattern in ω_1, as in the ω_2 dimension. This may be readily verified from the 2D contour plot where the ω_1 and ω_2 frequencies are correlated symmetrically with respect to the 45° diagonal. The 2D contour is also seen to extend over the frequency range covered by the powder pattern. The steps ($\theta = 90°$) and shoulders ($\theta = 0°$) of the powder pattern occur at the frequencies $(\omega_1,\omega_2) = \pm(e^2Qq/2h)P_2 \cos\theta$ and enable us to estimate (e^2Qq/h) to be 90 kHz, in good agreement with 1D measurements.[13]

3.4. 2-D Separation in $La_2Li_{0.5}Ni_{0.5}O_4$. The 2D spin echo separation of the quadrupolar spectrum in the paramagnetic layered oxide system $La_2Li_{0.5}Ni_{0.5}O_4$ is shown in Figure 3. As in the diamagnetic compound, the contour plot correlates the spectral frequencies in ω_2 with those in ω_1. The projections along ω_2 and ω_1 are also shown. As seen, the ω_2 projection gives rise to the normal 1D asymmetric ^{7}Li spectral pattern, while the ω_1 projection gives rise to a clean quadrupolar spectrum free from paramagnetic dipolar interactions. Since the π pulse in the 2D SE sequence refocuses the isotropic chemical shift, the ω_1 projection spectrum is centered at $\omega_1 = 0$. This central line is flanked by satellites due to the ($\pm$1/2 $\leftrightarrow$ $\pm$3/2) spin transitions, the steps and shoulders of which appear at $\pm$23.2 and $\pm$46.4 kHz, for the orientation of the unique axis of the electric field gradient tensor perpendicular ($\theta = 90°$) and parallel ($\theta = 0°$) to H_0, respectively. The frequency measurements at these unique orientations lead to an estimate of the quadrupole coupling constant (e^2qQ/h) for ^{7}Li in $La_2Li_{0.5}Ni_{0.5}O_4$ to be 92 kHz, in good agreement with the value of 89 kHz noted for the diamagnetic counterpart $La_2Li_{0.5}Cu_{0.5}O_4$. This results also shows that the ^{7}Li quadrupolar interaction is not significantly changed in the presence of Ni^{3+}.

The ω_1 and ω_2 frequencies are asymmetrically correlated with respect to the diagonal of slope = 1 due to the influence of Li$-$Ni paramagnetic dipolar interactions. Since a full 2D contour simulation is formidable and is beyond the scope of the present study, we merely identify the paramagnetic frequency shift of the steps and shoulders for the pair of satellites due to ($\pm$1/2 $\leftrightarrow$ $\pm$3/2) transitions appearing in the pure quadrupole spectrum

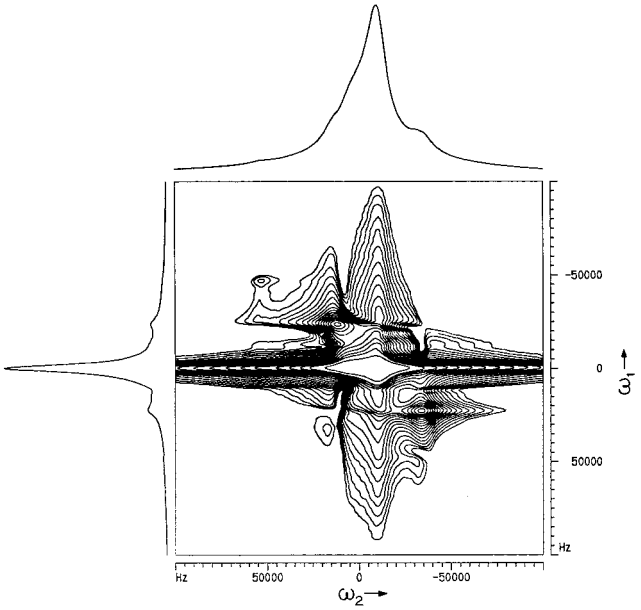

Figure 3. ^{7}Li 2D spin echo (SE) contour plot of $La_2Li_{0.5}Ni_{0.5}O_4$, obtained with a static sample. A 512 (t_1) × 1024 (t_2) 2D data matrix was acquired using 250 kHz spectral width, 2 μs t_1 increment, 0.15 s relaxation delay, and 800 scans. The 2D data set was apotized with an exponential line broadening, in the t_1 and t_2 dimensions prior to Fourier transformation. The ω_2 and ω_1 projections are also shown.

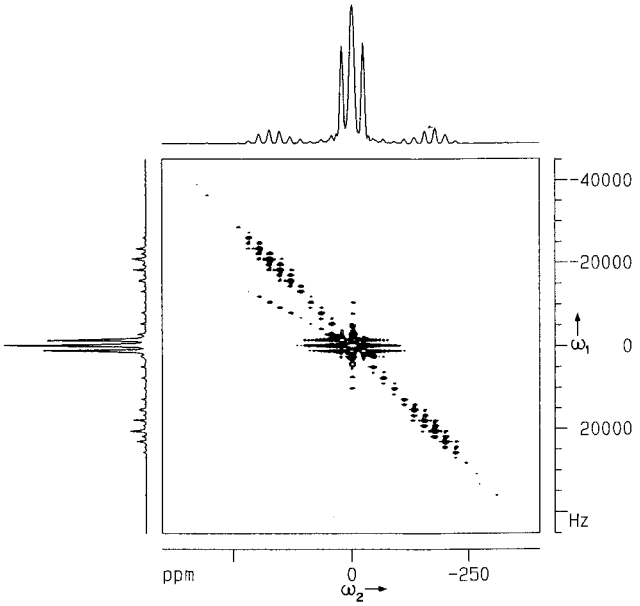

Figure 4. ^{7}Li MASS SE 2D contour plot of $La_2Li_{0.5}Cu_{0.5}O_4$ at the spinning speed of 2.57 kHz. A 512 (t_1) × 1024 (t_2) 2D data matrix was aquried using 125 kHz spectral width, 4 μs t_1 increment, 1 s relaxation delay, and 32 scans. The 2D data set was zero filled to 1024 points in the t_1 dimension and apotized using sine squared bell function in both the dimensions. The ω_2 and ω_1 projections are also shown.

along ω_1, and use the following expressions to estimate the angle between the efg and dipolar axes. Using the theoretical treatment of France,[4] we have

$$\delta P = \nu_{pc} - {}^1/_2(\nu_{shl} + \nu_{shh}) \quad (6)$$

$$\delta S = \nu_{pc} - {}^1/_2(\nu_{stl} + \nu_{sth}) \quad (7)$$

$$\tan^2 \Omega = 3\delta P/\delta S \quad (8)$$

The orinetation between the efg and dipolar tensors is contained in the angle Ω, which is estimated from eqs 6−8. Here, ν_{pc} corresponds to the position of the central transition peak and $^1/_2(\nu_{stl} + \nu_{sth})$ and $^1/_2(\nu_{shl} + \nu_{shh})$ correspond to the middle positions between steps and shoulders, respectively, corresponding to the satellite transition. From the 2D correlation provided by Figure 3, we estimate the various values as ν_{stl}, $\nu_{sth} = -57.3$, 50.2 kHz; ν_{shl}, $\nu_{shh} = -14.3$, 33.0 kHz; $\nu_{pc} = -11.0$ kHz, leading to the determination of 30° for Ω.

4. 2D Separation under MASS

In a static sample, in which the frequency, $\Delta\omega$, may have an orientation dependence but no time dependence, a single π pulse at time τ induces a spin echo at time 2τ. In rotating samples, it is well-known that these echo phenomena are more complicated because of time dependence of the precession frequency $\Delta\omega(t)$. The interference of π pulses with rotational echo phenomena has been already illustrated.[22] Depending upon its timing, the π pulse may induce its own spin echo or may interfere with the formation of the rotational echoes from the intrinsic time dependence of $\Delta\omega(t)$. The rotational echoes are produced in $\langle S(t_1,t_2)\rangle$ for t_2 equal to any integer multiple of τ_r, while t_1 must be an even integer multiple of τ_r. This $2\tau_r$ periodicity produces rotational sidebands in the F_1 dimension at half-integer multiples of spinning frequency.[23] The 2D spin echo techniques for measuring small chemical shielding anisotropies involve a single π pulse applied at the center of the evolution period, t_1. The resulting spectra have sidebands spaced at one-half of the spinning speed in the ω_1 dimension and for small anisotropies are much larger than the corresponding one-dimensional spectrum. The effect is similar to that of spinning the sample at one-half of the actual spinning speed, ω_r. A single π pulse at the center of the evolution period of the 2D dipolar chemical shift sequence, yields dipolar sidebands at $\omega_r/2$ with the frequency axis reversed and enhanced intensity to those from the 2D dipolar chemical shift experiment.[23,24]

It was observed that the ^{7}Li NMR spectra of $La_2Li_{0.5}$, $Cu_{0.5}O_4$, and $La_2Li_{0.5}Ni_{0.5}O_4$ (parts a and b of Figure 1) could be effectively narrowed by the magic-angle sample spinning (MASS).[13] At moderate spinning speeds (ca 3 kHz), the anisotropic powder pattern breaks into a series of spinning sidebands, whose envelope to a first approximation maps the static line shape. In an attempt to separate the quadrupolar interaction along the ω_1 dimension, we have also extended the 2D spin echo experiment under MASS conditions. The 2D contour plot for $La_2Li_{0.5}Cu_{0.5}O_4$ is shown in Figure 4. As in the case of a static sample, the 2D separation leads to the same quadrupolar patterns along ω_1 and ω_2 with an intense sideband pattern appearing in both the dimensions. Since rotor synchronization is not applied along t_1 and t_2, the sideband appear in both the dimensions. Here, a magnitude mode FT has been used to remove the dispersive effects on the sideband intensities. The sideband patterns imply a τ_r periodicity with respect to t_2, but a $2\tau_r$ periodicity with respect to t_1. As expected,[23] the effect of π pulse leads to the appearance of sidebands at $\omega_r/2$. The overall anisotropy due to first-order quadrupolar interaction, seen in the ω_1 projection spectrum, is unchanged in the MASS experiment. This allows us to estimate the quadrupole interaction parameters from the 1D MASS projection spectrum as well, in a manner similar to the nonspinning experiment. These were found to be close agreement with the quadrupole coupling constant estimated from the static experiments.

We show in Figure 5 a 2D contour plot for $La_2Li_{0.5}Ni_{0.5}O_4$ obtained under MASS. The ω_1 and ω_2 projections are also shown. The intense and asymmetric sideband profile for the ω_2 projection spectrum is similar to that observed in the normal

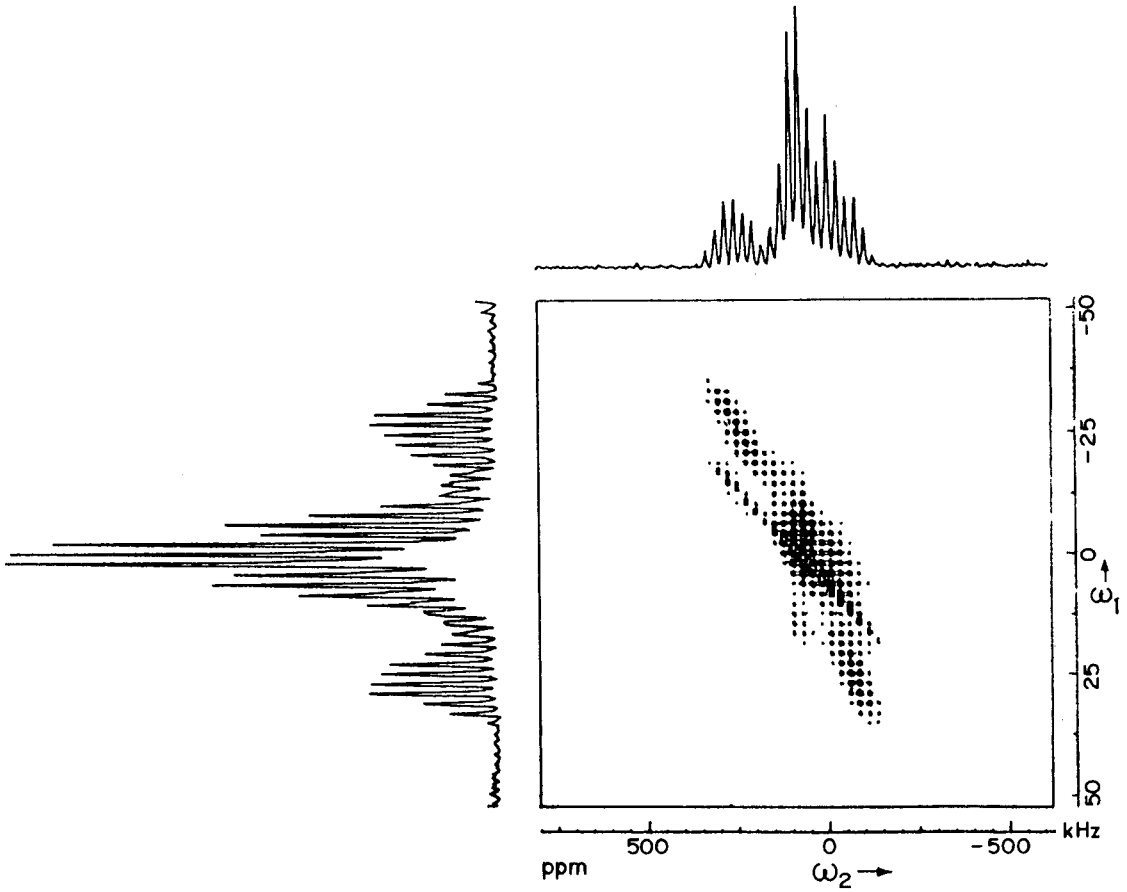

Figure 5. ^{7}Li MASS SE 2D contour plot of $La_2Li_{0.5}Ni_{0.5}O_4$ at the spinning speed of 2.55 kHz. A 256 (t_1) × 1024 (t_2) 2D data matrix was aquried using 200 kHz spectral width, 2.5 μs t_1 increment, 250 ms relaxation delay, and 40 scans. The 2D data set was zero filled to 1024 points in the t_1 dimension and apotized using sine squared bell function in both the dimensions. The ω_2 and ω_1 projections are also shown.

1D MAS spectrum of this compound.[13] The sideband profile in the ω_1 projection spectrum is symmetric about $\omega_1 = 0$, showing thereby the removal of the anisotropic paramagnetic interaction in the ω_1 dimension. Here also, the sidebands occur at half the spinning speed due to the $2\tau_r$ periodicity during t_1. From positions of the maximum satellite sideband intensities, we can readily estimate the quadrupole coupling constant from the ω_1 projection spectrum. We find this value of 92 kHz measured from the static 2D SE experiment.

5. Conclusions

The separation of ^{7}Li quadrupolar interaction in a system experiencing quadrupolar and anisotropic magnetic dipolar interactions has been achieved by employing a spin echo 2D experiment. The application of this method is demonstrated under static and MASS conditions on the paramagnetic layered oxide $La_2Li_{0.5}Ni_{0.5}O_4$. The ^{7}Li quadrupolar spectrum along the ω_1 dimension allows a direct measurement of the quadrupole coupling constant to be made in this paramagnetically broadened layered oxide. The utility of the 2D SE technique to other spin $((2n + 3)/2)$ nuclei in paramagnetic systems may be envisaged. It would be interesting to compare our results with the 2D ^{7}Li NMR of nickel oxycarbonates $Sr_2Li_{0.5}Ni_{0.5}O_2.CO_3$, which has the same basal plane $LiNiO_2$ structure as in $La_2Li_{0.5}Ni_{0.5}O_4$. This is currently being pursued, and the details will be published in another communication.

Acknowledgment. We thank Professor K. V. Ramanathan of SIF, IISc, Bangalore for valuable discussions.

References and Notes

(1) Baugher, J. F.; Taylor, P. C.; Oja, T.; Bray, P. J. *J. Chem. Phys.* **1969**, *50*, 4914. Taylor, P. C.; Baugher, J. F.; Kriz, H. M. *Chem. Rev.* **1975**, *75*, 203.

(2) Power, W. P.; Washylishen, R. E.; Mooibroak, S.; Pettitt, B. A.; Danchura, W. *J. Phys. Chem.* **1990**, *94*, 591.

(3) Siminovitch, D. J.; Rance, M.; Jeffrey, K. R.; Brown, M. F. *J. Magn. Reson.* **1984**, *58*, 64.

(4) France, P. W. *J. Magn. Reson.* **1991**, *92*, 30.

(5) Ernst, R. R.; Bodenhausen, G.; Wokaun, A. *Principles of Nuclear Magnetic Resonance in Two Dimensions*; Clarendon Press: Oxford, 1987. Power, W. P.; Washylshen, R. E. *Ann. Rep. NMR Spec.* **1991**, *23*, 1.

(6) Linder, M.; Hohener, A.; Ernst, R. R. *J. Chem. Phys.* **1980**, *73*, 4959. Nakai, T.; McDowell, C. A. *J. Am. Chem. Soc.* **1994**, *116*, 6373 and the references therein.

(7) Zilm, K. W.; Webb, G. G.; Cowley, A. H.; Pakulki, M.; Orendt, A. *J. Am. Chem. Soc.* **1988**, *110*, 2032.

(8) Einarsson, I.; Norendenskiold, L.; Rupprecht, A. *J. Magn. Reson.* **1991**, *93*, 34.

(9) Furo, I.; Halle, B.; Per-Ola Quist; Wong, T. C. *J. Phys. Chem.* **1990**, *94*, 2600.

(10) Dolinsek, J. *J. Magn. Reson.* **1991**, *92*, 312.

(11) Sponiol, T. P.; Kubo, A.; Terao, T. *J. Chem. Phys.* **1997**, *106*, 5393.

(12) Shore, J. S.; Wang, S. H.; Taylor, R. E.; Bell, A. T.; Pines, A. *J. Chem. Phys.* **1996**, *105*, 9412.

(13) Ganguly, P.; Venkatraman, T. N.; Pradhan, S.; Rajamohanan, P. R.; Ganapathy, S. *J. Phys. Chem.* **1996**, *100*, 5017.

(14) Carr, H. Y.; Purcell, E. M. *Phys. Rev.* **1954**, *94*, 630.

(15) Meiboom, S.; Gill, D. *Rev. Sci. Instrum.* **1958**, *29*, 688.

(16) Hoult, D. I.; Richards, R. E. *Proc. R. Soc. Ser.* A **1975**, *344*, 311.

(17) Abragam, A. *Principles of Nuclear Magnetism*; Oxford University Press: London, 1961.

(18) Bloembergan, N. *Physica* **1950**, *16*, 95.

(19) Woehler, S. E.; Wittebort, R. J.; Oh, S. E.; Hendrikson, D. N.; Inniss, D.; Strouse, C. E. *J. Am. Chem. Soc.* **1986**, *108*, 2938.

(20) Davis, J. H.; Jeffrey, K. R.; Bloom, M.; Valic, I.; Higgs, T. P. *Chem. Phys. Lett*. **1976**, *42*, 390.

(21) Gerothanassis, I. P. *Prog. NMR. Spectrosc.* **1987**, *19*, 267 and the references therein.

(22) Olejniczak, E. T.; Vega, S.; Griffin, R. G. *J. Chem. Phys.* **1984**, *81*, 4804.

(23) Kolbert, A. C.; Raleigh, D. P.; Levitt, M. H.; Griffin, R. G. *J. Chem. Phys.* **1989**, *90*, 679.

(24) Kolbert, A. C.; Griffin, R. G. *J. Magn. Reson.* **1991**, *93*, 242.